Chemico-Biological Interactions 183 (2010) 142–153

Contents lists available at ScienceDirect

Chemico-Biological Interactions

journal homepage: www.elsevier.com/locate/chembioint

2′-epi-2′-O-Acetylthevetin B extracted from seeds of *Cerbera manghas* L. induces cell cycle arrest and apoptosis in human hepatocellular carcinoma HepG2 cells

Bo Feng[a], Yue-Wei Guo[b], Cai-Guo Huang[a,*], Liang Li[b], Ruo-Hua Chen[c], Bing-Hua Jiao[a,*]

[a] Department of Biochemistry and Molecular Biology, Second Military Medical University, 800 Xiangyin Road, Shanghai 200433, PR China
[b] State Key Laboratory of Drug Research, Shanghai Institute of Materia Medica, Chinese Academy of Sciences, Shanghai 201203, PR China
[c] Changhai Hospital, Shanghai 200433, PR China

ARTICLE INFO

Article history:
Received 4 April 2009
Received in revised form 12 October 2009
Accepted 16 October 2009
Available online 27 October 2009

Keywords:
2′-epi-2′-O-Acetylthevetin B (GHSC-74)
Cell cycle arrest
Mitochondrial membrane potential ($\Delta\Psi_m$)
Apoptosis-inducing factor (AIF)
Reactive oxygen species (ROS)
Caspase
Apoptosis

ABSTRACT

2′-epi-2′-O-Acetylthevetin B (GHSC-74) is a cardiac glycoside isolated from the seeds of *Cerbera manghas* L. We have demonstrated that GHSC-74 reduced the viability of HepG2 cells in a time- and dose-dependent manner. The present study was designed to explore cellular mechanisms whereby GHSC-74 led to cell cycle arrest and apoptosis in HepG2 cells. Cell cycle flow cytometry demonstrated that HepG2 cells treated with GHSC-74 (4 μM) resulted in S and G2 phase arrest in a time-dependent manner, as confirmed by mitotic index analysis. G2 phase arrest was accompanied with down-regulation of CDC2 and Cyclin B1 protein. Furthermore, GHSC-74-induced apoptotic killing, as demonstrated by DNA fragmentation, DAPI staining, and flow cytometric detection of sub-G1 DNA content in HepG2 cells. GHSC-74 treatment resulted in a significant increase in reactive oxygen species, activation of caspase-9, dissipation of mitochondrial membrane potential, and translocation of apoptosis-inducing factor (AIF) from the mitochondrion to the nucleus in HepG2 cells. Nevertheless, after GHSC-74 exposure, no significant Fas and FasL up-regulation was observed in HepG2 cells by flow cytometry. In addition, treatment with antioxidant N-acetyl-L-cysteine (NAC) and broad-spectrum caspase inhibitor z-VAD-fmk partially prevented apoptosis but did not abrogate GHSC-74-induced nuclear translocation of AIF. In conclusion, we have demonstrated that GHSC-74 inhibited growth of HepG2 cells by inducing S and G2 phase arrest of the cell cycle and by triggering apoptosis via mitochondrial disruption including both caspase-dependent and -independent pathways, and ROS generation.

1. Introduction

2′-epi-2′-O-Acetylthevetin B (GHSC-74) (Fig. 1) is isolated from the seeds of *Cerbera manghas* L. [1], belonging to the class of steroid-like compounds designated as cardiac glycosides. Their continued efficacy in the treatment of congestive heart failure and dysrhythmia is well appreciated [2]. However, there is little knowledge about the role of this category of compounds in the prevention and/or treatment of proliferative diseases such as cancer. New findings in recent five years have demonstrated that these compounds are involved in complex cell-signal transduction mechanisms, inducing selective control of human tumors rather than normal cellular proliferation [3,4], and as such represent a promising candidate for targeted cancer chemotherapy.

Hepatocellular carcinoma (HCC) is generally acknowledged as the sixth most prevalent cancer in the word and is currently the third most common cause of cancer death with a 5-year survival rate of 7% [5–7]. Hepatic resection and liver transplantation are the two mainstays of curative treatment for HCC, but can only be applied to the early stage of HCC [8]. The majority of patients with HCC are diagnosed at a late stage when curative treatment options are not applicable. Thus, developing new therapeutic and preventive strategies targeted at apoptosis inducing could be effective in controlling the proliferation and invasiveness as well as in the prognosis advanced stages of HCC.

Many cytotoxic agents and/or DNA damaging agents arrest cell cycling at G1, S or G2/M phase, inducing apoptotic cell death [9,10]. Cell cycle checkpoints may function to ensure cells to have time for DNA repair [11,12]. In recent years, considerable advances have been made in understanding the roles of cyclins and cyclin-dependent kinases (Cdks) in cell cycle progression. This process is regulated by the coordinated action of Cdks in association with their specific regulatory cyclin proteins [12]. G2 to M phase progression is regulated by a number of the Cdk/cyclin family members. Activation of Cdk1/cyclin B1 complex is required for transition from G2 to M phase of the cell cycle [13,14]. CDC2 is a catalytic subunit of the highly conserved protein kinase complex known as M-phase pro-

* Corresponding authors. Tel.: +86 21 81870970 8020; fax: +86 21 65334344.
E-mail addresses: huangcaiguo@hotmail.com (C.-G. Huang), jiaobh@uninet.com.cn (B.-H. Jiao).

0009-2797/$ – see front matter © 2009 Elsevier Ireland Ltd. All rights reserved.
doi:10.1016/j.cbi.2009.10.012

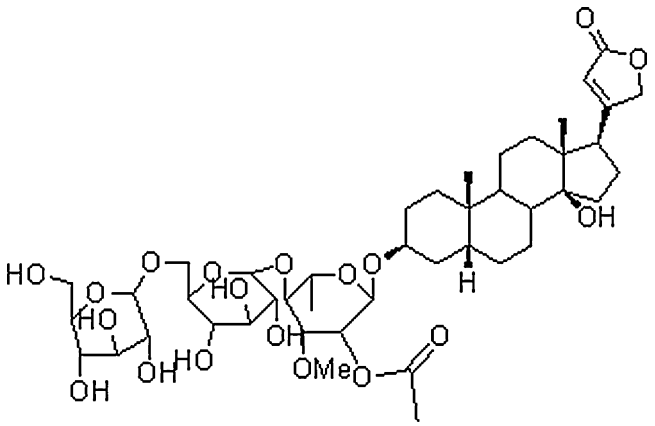

Fig. 1. Chemical structure of GHSC-74.

moting factor (MPF), which is essential for G1/S and G2/M phase transitions of the eukaryotic cell cycle. Mitotic cyclins stably associate with this protein and function as regulatory subunits. The kinase activity of this protein is controlled by cyclin accumulation and destruction through the cell cycle. Phosphorylation and dephosphorylation of this protein also play important regulatory roles in cell cycle control [15].

Until recently, two major apoptotic pathways, the death receptor pathway and the mitochondrial apoptotic pathway, are well characterized in mammalian cells [16]. The death receptor pathway is triggered by members of the death receptor family, such as Fas receptor and tumor necrosis factor receptor [17]. Binding of Fas ligand (FasL) to Fas receptor induces receptor clustering and the formation of a death-inducing signaling complex, which in turn recruits and activates caspase-8, as an initiator caspase, via the adaptor molecule Fas-associated death domain protein (FADD) [18]. On the other hand, mitochondrial membrane permeabilization is considered to be one of the initial events of the apoptotic process induced by chemotherapeutic drugs [19]. Cytochrome c and apoptosis-inducing factor (AIF) are well known as proapoptotic molecules released from the mitochondria [20,21]. Cytochrome c is usually released from the mitochondrial intermembrane space into the cytosol as consequence of the mitochondrial membrane potential ($\Delta\Psi_m$) loss [20,22]. Cytochrome c released from the mitochondria forms a complex with procaspase-9 and apoptotic protease-activating factor-1 (Apaf-1), resulting in activation of procaspase-9. Contrarily, AIF condenses chromatin to induce apoptosis without involving caspases. Although the mechanism of AIF release from the mitochondria has not been fully understood, the regulatory role of AIF during programmed cell death has been well documented. AIF is a putative caspase-independent effector of cell death, and has recently been characterized as proapoptotic mitochondrial intermembrane flavoprotein [21,23]. Similar to cytochrome c, AIF is released from the mitochondria in response to death stimuli. On induction of apoptosis, AIF is translocated to the nucleus and causes large-scale DNA fragmentation and chromatin condensation in a caspase-independent manner [21,23].

Reactive oxygen species (ROS) are highly reactive O_2 metabolites, including superoxide radical ($O_2^{-\bullet}$), hydrogen peroxide (H_2O_2), and hydroxylradical (OH^-) [24]. These molecules have recently been implicated in the regulation of many important cellular events, including transcription factor activation, gene expression, differentiation, and cellular proliferation [25,26]. Although cells possess antioxidant systems to control the redox state, which is important for their survival, high levels of ROS can lead to necrotic cell death, and low levels of ROS have been shown to induce apoptotic cell death [27].

We have demonstrated that GHSC-74 reduced the viability of HepG2 cells in a time- and dose-dependent manner with an IC_{50} (median growth inhibitory concentration value) of approximately 3.66 μM, 0.66 μM and 0.41 μM following treatment with GHSC-74 for 24 h, 48 h and 72 h, respectively [28]. This study was designed to identify possible anti-proliferative effects of GHSC-74 in HepG2 cells. Our data showed that GHSC-74 inhibited the growth of HepG2 cells by inducing S and G2 arrest of the cell cycle and by triggering apoptosis via mitochondrial disruption including both caspase-dependent and -independent pathways, and ROS generation.

2. Materials and methods

2.1. Reagents

Reagents used in the present study included Minimal Essential medium (MEM), fetal bovine serum (FBS), penicillin, streptomycin, trypsin-EDTA (GIBCO Laboratories, Grand Island, USA); Propidium iodide (PI), Dimethylsulfoxide (DMSO), paraformaldehyde, N-acetylcysteine (NAC), Triton X-100, RNAase A (Sigma Chemical Co., St. Louis, USA); Fluorescein isothiocyanate (FITC)-conjugated antihuman Fas antibody (DX2), phycoerythrin (PE)-conjugated antihuman FasL antibody (Biolegend, San Diego, CA); 2′,7′-dichlorofluorescin diacetate (DCFH/DA) (Invitrogen Molecular Probes, Eugene, OR); JC-1 (The probe 5,5′,6,6′-tetrachloro-1,1′,3,3′-tetraethyl-benzimidazolcarbocyanine iodide) Detection Kit (Molecular Probes); 4′, 6-diamidino-2-phenylindole (DAPI) (Roche, Indianapolis, IN); Giemsa (LabChem Inc., Pittsburgh, PA); Antibody specific polyclonal AIF, Cy3-conjugated anti-rabbit IgG secondary antibody, anti-CDC2, anti-Cyclin B1 (Santa Cruz Biotechnology, Santa Cruz, CA, USA); broad-spectrum caspase inhibitor N-benzyloxycarbonyl-Val-Ala-Asp-fluoromethylketone (z-VAD-fmk) (Calbiochem, San Diego, CA). Caspase-9 Colorimetric Assay Kits (R&D systems Inc., Minneapolis, MN); all other chemicals were of analytical grade.

2.2. Test compound

GHSC-74 (purity ≥95% by ^{1}H Nuclear Magnetic Resonance (NMR) spectroscopy and Liquid Chromatography–Mass Spectrum (LC-MS)) was purified by Shanghai Institute of Materia Medica, the Chinese Academy of Sciences according to the previously described method (Abe and Yamauchi [1]). Briefly, fresh seeds (1.3 kg, dry weight) of *C. manghas* L. were cut into pieces and extracted exhaustively with MeOH (3 l × 15 l). The MeOH extract was concentrated *in vacuo* to give a residue which was dissolved in H_2O (1000 ml) and the solution was partitioned consecutively between H_2O and petroleum ether, H_2O and EtOAc, H_2O and *n*-BuOH. The *n*-BuOH extract (62 g) was separated by column chromatography (CC) on silica gel (100–200 mesh). The column was eluted with a gradient of chloroform-MeOH (9:1–0:100) to give 6 fractions (Fr.1–Fr.6) on the basis of TLC checking. Fraction 3 (17.0 g) was further purified by Sephadex LH-20 (chloroform/MeOH 1:1), followed by CC on silica gel and eluted with a gradient of chloroform-MeOH (9:1–3:2) to give GHSC-72 (9.0 mg), GHSC-74 (187 mg), GHSC-75 (870 mg) and GHSC-79 (12 mg).

2.3. Cell culture and drug preparation

Human HCC cell line HepG2 was purchased from the cell bank of Shanghai Institute of Cell Biology (Shanghai, China). HepG2 cells were maintained in MEM containing 10% heat-inactivated FBS, and 100 U/ml penicillin + 100 μg/ml streptomycin. Cells were grown in a 37 °C incubator supplied with 95% room air and 5% CO_2. After growing to 60–80% confluency, cells were trypsinized with 0.25% trypsin-EDTA, counted, and placed down at the desired density for

treatment. GHSC-74 was dissolved in DMSO and further diluted in PBS. The final DMSO concentration was 0.1%, which did not affect cell function and the assay systems.

2.4. Assessment of cell cycle distribution and sub-G1

Cell cycle and sub-G_1 distribution were determined by staining DNA with PI as previously described [29]. Briefly, HepG2 cells were plated at a density of 1×10^6 cells/well. After treatment, cells were collected, washed twice with ice-cold PBS buffer (pH 7.4), fixed with 70% alcohol at 4 °C overnight, and then stained with PI (1 mg/ml) in the presence of 1% RNAase A for at least 30 min. The percentage of cells in different phases of the cell cycle or having the sub-G1 DNA content were measured with a FACScalibur flow cytometer (Becton Dickinson, San Jose, CA).

2.5. DNA fragmentation analysis

HepG2 cells (2×10^6 cells/ml) under different treatments were collected, washed with PBS twice and then lysed in 100 μl lysis buffer [50 mM Tris (pH 8.1); 10 mM EDTA; 0.5% sodium sarkosinate and 1 mg/ml proteinase K] for 3 h at 56 °C and treated with RNase A (0.5 μg/ml) for another hour at 37 °C. DNA was extracted by phenol: chloroform: isoamyl alcohol (v/v/v, 25:24:1) before loading, and analyzed by 1.8% agarose gel electrophoresis in the presence of 0.1 μg/ml ethidium bromide (EtBr). The agarose gel was run at 50 V for 90 min in Tris-borate/EDTA electrophoresis buffer (TBE). Approximately 30 μg DNA was loaded in each well and visualized under UV light and photographed.

2.6. DAPI staining for nuclear condensation and fragmentation

HepG2 cells were treated with 4 μM GHSC-74 for 48 h. Cells were fixed with 1% paraformaldehyde on slide glass for 30 min at room temperature. After washing with PBS, 300 nM DAPI was added to the fixed cells for 5 min, and examined by fluorescence microscopy (Olympus, IX70, Japan). Apoptotic cells were identified by nuclear condensation and fragmentation. The DAPI staining experiments were done in duplicate.

2.7. Mitotic index assay

For assessment of the mitotic index, cells treated with GHSC-74 (4 μM) or vehicle control were harvested, washed in ice-cold PBS, re-suspended in 0.5 × PBS (10 min), and fixed in 0.5 ml ethanol: acetic acid (3:1) for 10 min. The cell suspension was dropped onto glass slides, air dried, and stained with 5% (v/v) Giemsa solution. For each spread, at least 500 cells were randomly counted by light microscopy and mitotic cells were scored by their lack of nuclear membrane and evidence of chromosome condensation. The mitotic index was reported as the percentage of mitotic cells per total cell number of cells.

2.8. Mitochondrial membrane potential assay

The mitochondrial membrane potential was determined quantitatively by flow cytometry using the fluorescent lipophilic cationic probe JC-1 (The probe 5,5′,6,6′-tetrachloro-1,1′,3,3′-tetraethylbenzimidazolcarbocyanine iodide) Detection Kit following the manufacturer's instructions. JC-1 was selectively concentrated or accumulated within intact mitochondria to form multimer J-aggregates emitting fluorescence light at 590 nm. The monomeric form emits light at 527 nm after excitation at 490 nm. Thus, the color of the dye changes from red to green, depending on the mitochondrial membrane potential, and can be analyzed by FACS with green fluorescence in channel 1 (FL1) and red emission in channel 2 (FL2). Briefly, HepG2 cells were treated with GHSC-74 (4 μM) for 0 h, 24 h and 48 h, harvested, and washed with PBS. 1×10^6 cells were incubated in 1 ml PBS containing 10 μg JC-1 for 15 min at 37 °C in the dark. Stained cells were washed, re-suspended in 500 μl PBS, and analyzed on a flow cytometer (FACScalibur, Becton Dickinson).

2.9. Quantification of caspase-9 activity

Activity of caspase-9 was assessed using the caspase-9 Colorimetric Assay Kits, based on spectrophotometric detection of color reporter molecule detection *p*-nitroanaline (*p*NA) after cleavage from labeled substrate LEHD-*p*NA (caspase-9) as an index. In brief, cells were incubated with 4 μM GHSC-74 for various time periods, washed in PBS, and suspended in 5 volumes of lysis buffer (20 mM Hepes, pH 7.9, 20% Glycerol, 200 mM KCl, 0.5 mM EDTA, 0.5% NP40, 0.5 mM DTT, 1% protease inhibitor cocktail (Sigma). The lysate was then collected and stored at −20 °C until use. The protein concentration was determined by the Bradford method. Supernatant samples containing 100 μg total protein were determined for caspase-9 activity. They were added to each well in 96-well microtiter plates with LEHD-*p*NA at 37 °C for 1–2 h. The optical density of each well was measured at 405 nm using a microplate reader (Model 550, Bio-Rad, USA). Each plate contained multiple wells of a given experimental condition and multiple control wells. Activity of caspse-9 was expressed in arbitrary absorbance units (absorbance at a wavelength of 405 nm).

2.10. Localization of apoptosis-inducing factor (AIF) by immunofluorescence microscopy

Cells (5×10^4) were cytospun onto noncharged slides, fixed for 20 min in 4% paraformaldehyde, washed again with PBS, and permeabilized with 1% Triton X-100 for 30 min at room temperature and washed with TBS containing 0.1% sodium azide. To reduce nonspecific antibody binding, slides were incubated in 1% bovine serum albumin in TBS for 1 h at room temperature before incubation with rabbit polyclonal antibody to human AIF overnight at 4 °C. Slides were then washed for 30 min in TBS containing 0.1% sodium azide and incubated for 1 h with Cy3-conjugated secondary antibody. Nuclei were stained with 4′,6-diamidino-2-phenylindole for 15 min at room temperature. Slides were washed and air dried before they were mounted on coverslips with ProLong antifade mounting medium (Molecular Probes, Eugene, OR), and then examined under a fluorescence microscope (Olympus, IX70, Japan)

2.11. Detection of Fas/FasL by flow cytometry

Fas and FasL were measured by immunofluorescence flow cytometric analysis. After various treatments, a total of 1×10^6 cells was collected by centrifugation and washed twice with ice-cold PBS containing 1% BSA. Cells were then incubated with 100 μl fluorescein isothiocyanate (FITC)-conjugated anti-Fas antibody or phycoerythrin (PE)-conjugated anti-FasL antibody on ice for 40 min. After incubation in the dark, cells were washed twice and re-suspended in ice-cold PBS. Immunofluorescence staining of Fas and FasL was analyzed by FACS with green fluorescence in channel 1 (FL1) and red fluorescence in channel 2 (FL2), and calculated by CellQuest software.

2.12. Measurement of ROS generation

Cells were incubated in the absence or presence of GHSC-74 for the indicated time. 30 min before termination of the incubated period, 2′,7′-dichlorofluorescin diacetate (DCFH/DA) (10 μM) was added to cells and incubated for the last 30 min at 37 °C. Then, cells

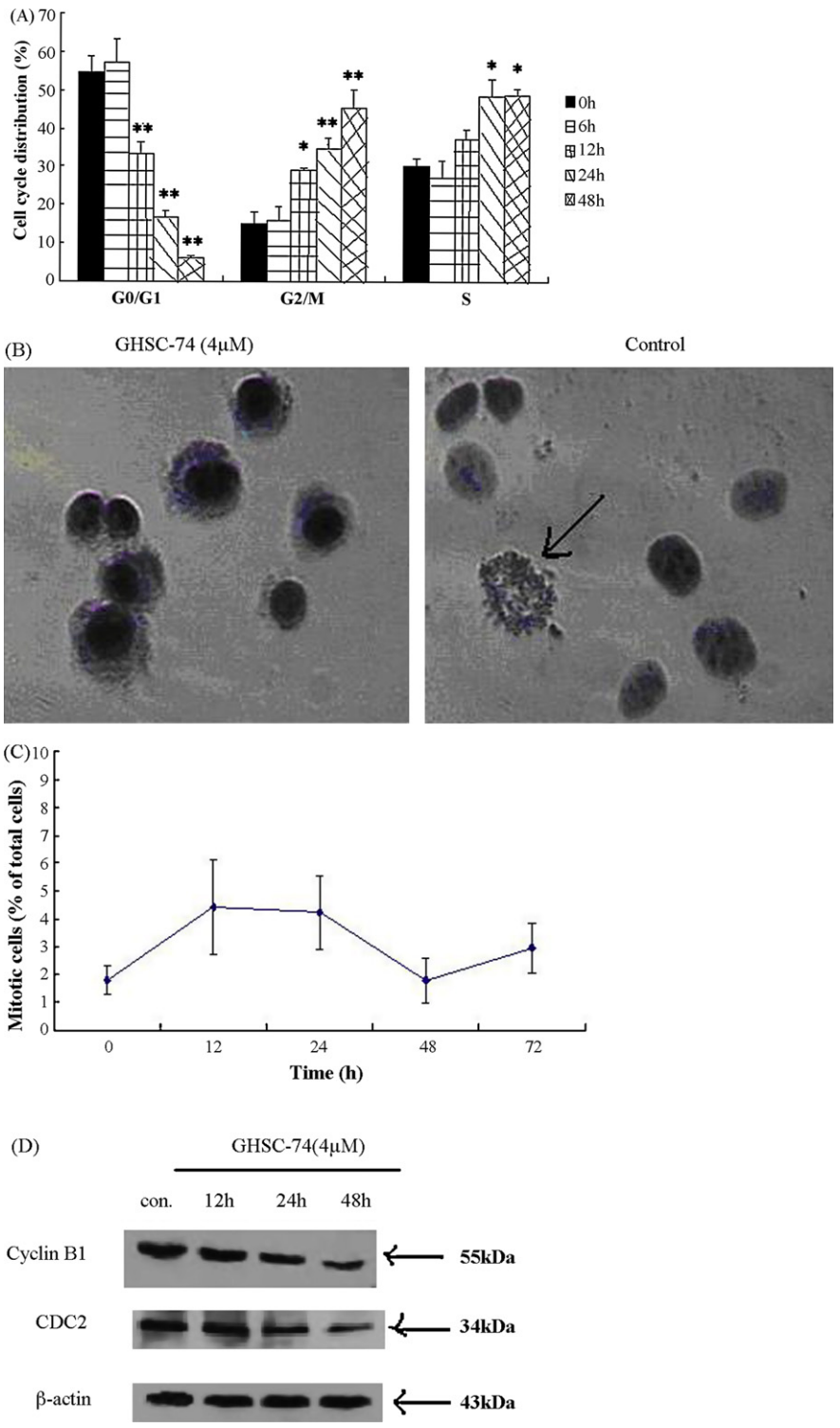

Fig. 2. Effect of GHSC-74 on cell cycle distribution in HepG2 cells. (A) HepG2 cells were treated with 4 μM GHSC-74 for various time periods by DNA flow cytometry. Histograms showed the number of cells per channel (vertical axis) vs. DNA content (horizontal axis). The values indicated the percentage of cells in the indicated phases of the cell cycle. (B) HepG2 cells treated with either 0.1% DMSO (control) or GHSC-74 (4 μM) for 48 h were harvested, washed, re-suspended in 0.5 × PBS, and fixed as described previously. Cell suspensions were dropped onto glass slides, air dried, and stained with Giemsa. Mitotic cells demonstrated the loss of nuclear membranes and chromosome condensation (arrow). (C) GHSC-74 arrest of HepG2 cells in G2 and before mitosis entry. HepG2 cells were treated with 4 μM GHSC-74 for various time periods by mitotic index assay. At least 500 cells were randomly counted by light microscopy. (D) Effects of GHSC-74 on cell cycle-related proteins in HepG2 cells. Exponentially growing cells were treated with 4 μM GHSC-74 for the indicated time periods. Aliquots of 50 μg protein extracts were resolved by 12% SDS-PAGE gel, transferred onto the NC membrane, and immunoblotted with the indicated antibodies, CDC2, Cyclin B1 and β-actin. Each value is the mean ± S.D. of three determinations. The asterisk indicates a significant difference between control and GHSC-74-treated cells as analyzed by Student's *t*-test ($^{*}p < 0.05$, $^{**}p < 0.01$).

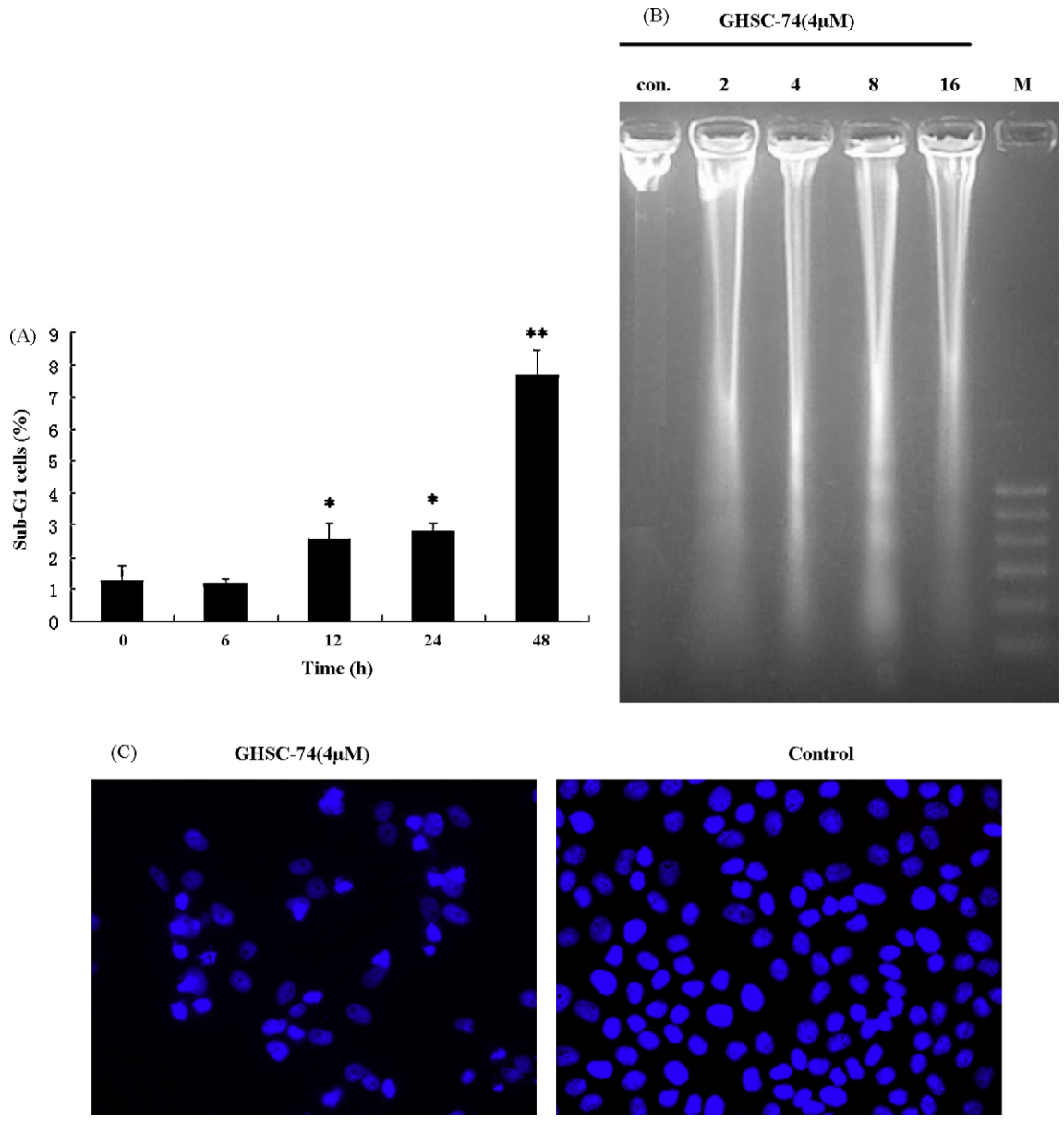

Fig. 3. GHSC-74-induced apoptosis in HepG2 cells. (A) GHSC-74-induced apoptosis in a time-dependent manner. HepG2 cells were treated with GHSC-74 (4 μM) with various time periods. Apoptosis was analyzed as a sub-G1 fraction by FACS. (B) DNA fragmentation analysis showing induction of apoptosis. HepG2 cells were treated with different concentrations of GHSC-74 as indicated for 48 h. M, 100 bp DNA marker; con, GHSC-74-untreated HepG2 cells. (C) Detection of GHSC-74-induced apoptosis in HepG2 cells by 4′,6-diamidino-2-phenylindole (DAPI) staining. Nuclear morphology was observed by fluorescence microscopy (magnification 200×). Each value is the mean ± S.D. of three determinations. The asterisk indicates a significant difference between control and GHSC-74-treated cells as analyzed by Student's *t*-test (*$p < 0.05$, **$p < 0.01$).

were harvested for detection of ROS accumulation using FACScalibur flow cytometric analysis, with an excitation wavelength of 480 nm and emission wavelength of 530 nm.

2.13. Preparation of mitochondrial and cytosolic fractions

Methods used for subcellular fraction were similar to those described previously [30].

2.14. Western blot analysis

Cells were scraped from the culture, washed twice with PBS, and then suspended in 30 μl Western blot lysis buffer containing 50 mM Tris–HCl (pH 7.5), 250 mM NaCl, 1 mM EDTA, 1 mM EGTA, 1 mM NaF, 1 mM phenylmethylsulfonyl fluoride, 1 mM DTT, 20 μg/ml leupeptin, 20 μg/ml aprotinin, 0.1% Trion X-100, and 1% SDS at 0–4 °C for 15 min. After centrifugation at 12,000 × *g* for 5 min at 4 °C, the supernatant was collected, and the protein concentration was determined using bicinchoninic acid (BCA) protein assay (Beyotime Biotechnology, Haimen, China). Equal amounts (50 μg protein) of lysate were subjected to 12% SDS-PAGE. After electrophoresis, protein blots were transferred to a nitrocellulose membrane using an electro-blotting apparatus (Bio-Rad). The membrane was blocked with 5% nonfat milk in TBST solution, and incubated overnight with the corresponding primary antibodies in the blocking solution at 4 °C. After three washes with TBST solution, the membrane was incubated at room temperature for 1 h, with horseradish peroxidase-conjugated secondary antibody diluted with TBST solution (1:3000). The signals of detected proteins were visualized by an enhanced chemiluminescence reaction (ECL) system (Amersham, ECL kits).

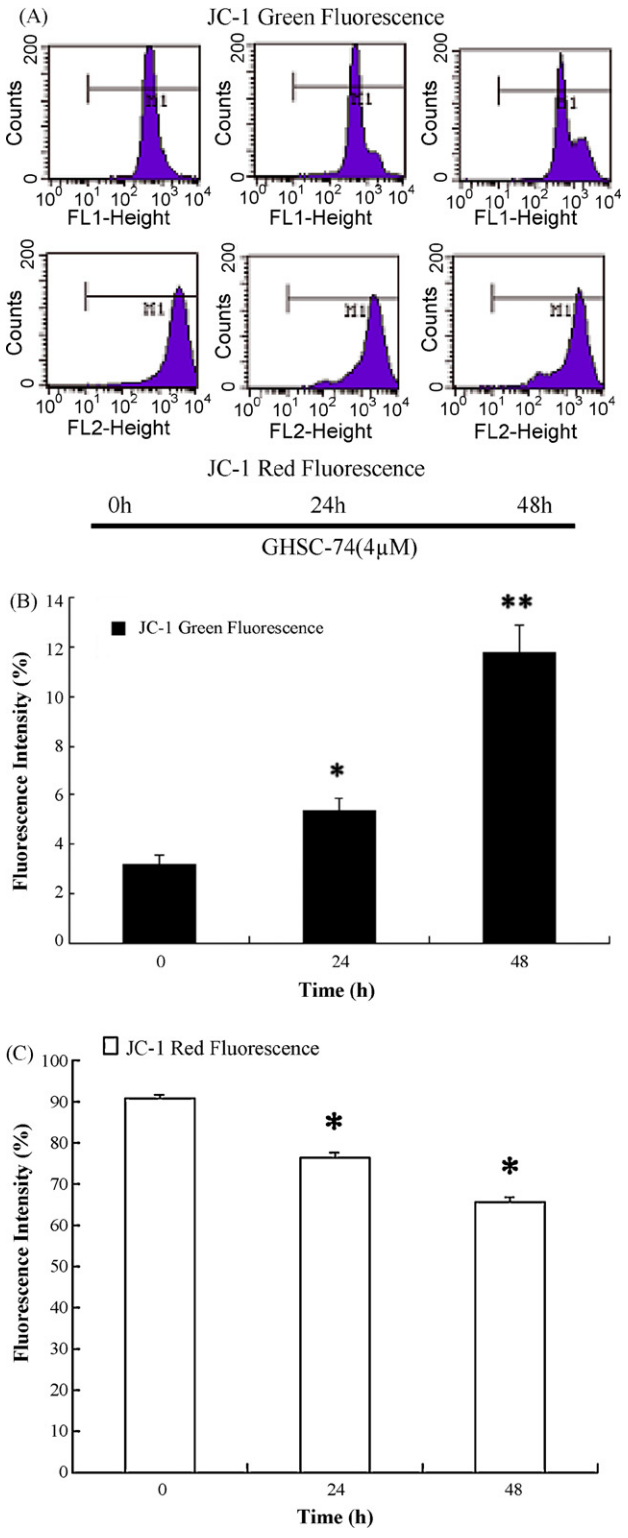

Fig. 4. Treatment of HepG2 cells with GHSC-74 induces loss of the mitochondrial membrane potential in a time-dependent manner. (A) The FACS representative graph for red fluorescence (indicator of intact mitochondrial membrane potential) and green fluorescence (indicator of mitochondrial membrane potential collapse) in HepG2 cells. (B) The percentage of the cells that emit green fluorescence indicates the depolarized mitochondrial membrane. (C) The percentage of the cells that emit red fluorescence indicate the intact mitochondrial membrane. Each value is the mean ± S.D. of three determinations. The asterisk indicates a significant difference between control and GHSC-74-treated cells as analyzed by Student's *t*-test (*$p < 0.05$, **$p < 0.01$). (For interpretation of the references to color in this figure legend, the reader is referred to the web version of the article.).

2.15. Statistical analysis

Data are reported as mean ± S.D. All experiments were done at least three times, and three or more independent observations were made on each occasion. Statistically significant values were compared using Student's *t*-test for single comparison and *p*-values less than 0.05 were considered statistically significant.

3. Results

3.1. Effect of GHSC-74 on cell cycle phase distribution

To explore the effect of GHSC-74 on cell cycle progression, HepG2 cells were incubated in the presence or absence of a 4 μM concentration of GHSC-74 for different time periods and then analyzed by flow cytometry. GHSC-74 caused a progressive increase in the population of cells in S-phase, an accumulation of cells in G2/M phase and a concomitant decrease in the percentage of cells in G0/G1 in time-dependent manner (Fig. 2A).

As Fluorescence-Activated Cell Sorting (FACS) analysis was unable to distinguish G2 phase cells from M-phase cells, we measured the mitotic index of cells after 4 μM GHSC-74 treatment to assess whether the mitotic apparatus may have been perturbed, thus explaining the increase in G2/M DNA content. As illustrated in Fig. 2B (right panel), the arrow indicates the loss of nuclear membrane and chromosome condensation, features that are typical of cell cycle arrest in metaphase. Most HepG2 cells exposed to either vehicle (Fig. 2B, right panel) or 4 μM GHSC-74 (Fig. 2B left panel) for 48 h showed intact nuclear membranes without an increase in mitotic figures. At the same time, Fig. 2C shows that the mitotic index in GHSC-74-treated cultures for different time periods was very low, indicating that increased G2/M DNA content provoked by GHSC-74 in HepG2 cells resulted from arrest of cells in G2 (interphase) preventing them from entering mitosis.

GHSC-74 seemed to trigger growth arrest in S and G2 phase of the cell cycle by modulation of cell cycle-regulatory proteins in HepG2 cells. CDC2 and Cyclin B1 protein levels, which are related to the progression of G2 phase, were down-regulated in a time-dependent manner in cells treated with GHSC-74 (4 μM) (Fig. 2D).

3.2. GHSC-74 induces apoptosis in HepG2 cells

HepG2 cells were treated with GHSC-74 (4 μM) for the indicated time periods. Apoptosis in HepG2 cells was first determined by flow cytometric analysis to count hypodiploid cell populations. As shown in Fig. 3A, treatment of HepG2 cells with GHSC-74 resulted in a marked increase in accumulation of sub-G1 phase cells in a time-dependent manner.

We also analyzed whether DNA fragmentation, another hallmark of apoptosis, was induced by GHSC-74 in HepG2 cells. Following agarose gel electrophoresis of HepG2 cells treated with 0 μM, 2 μM, 4 μM, 8 μM and 16 μM GHSC-74 for 48 h, a typical ladder pattern of internucleosomal fragmentation was not evident (Fig. 3B).

Cell morphology was also assessed by DAPI staining. As shown in Fig. 3C, the nuclear structure of control cells remained intact, while nuclear chromatin condensation and fragmentation, a characteristic of apoptosis, was seen in cells treated with 4 μM GHSC-74 for 48 h.

3.3. Essential role of mitochondria in GHSC-74-induced apoptosis

To study the potential effects of GHSC-74 on the mitochondrial apoptotic pathway, the mitochondrial membrane potential ($\Delta\Psi_m$) in HepG2 cells treated with GHSC-74 was measured, where

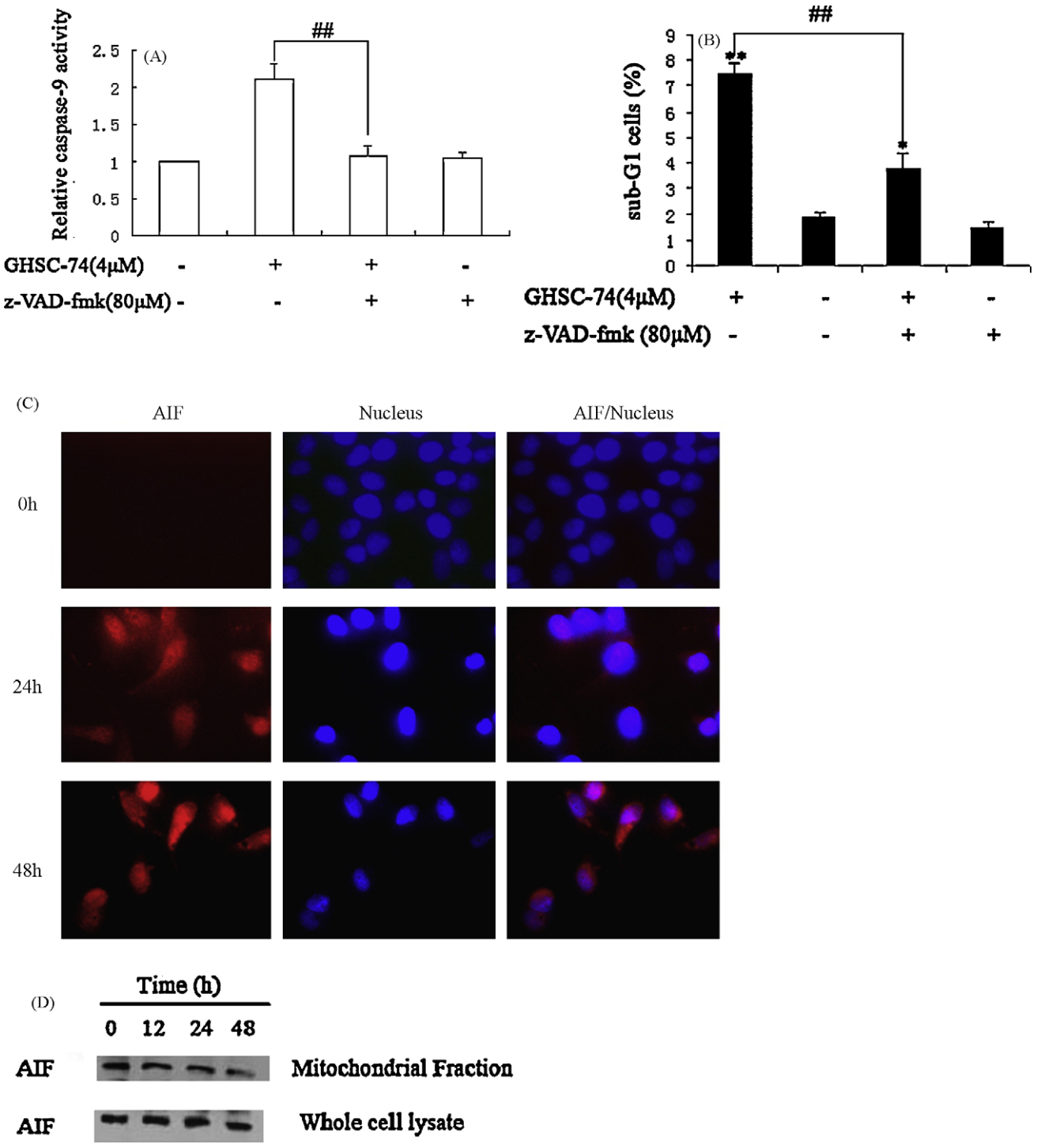

Fig. 5. GHSC-74 induces apoptosis of HepG2 cells through mitochondrial disruption including both caspase-dependent and- independent pathways. (A) Caspase-9 activity was determined as described in Section 2. HepG2 cells were treated with broad-spectrum caspase inhibitor z-VAD-fmk for 1 h before adding GHSC-74 (4 μM) for another 48 h. "#" indicates a significant difference between GHSC-74 group and GHSC-74+z-VAD-fmk group, as analyzed by Student's *t*-test (##$p < 0.01$). (B) Broad-spectrum caspase inhibitor z-VAD-fmk partially inhibited GHSC-74-induced apoptosis. HepG2 cells were treated with z-VAD-fmk for 1 h before adding GHSC-74 (4 μM) for another 48 h. Apoptosis was measured by the PI method using flow cytometry. "#" indicates a significant difference between GHSC-74 group and GHSC-74+ z-VAD-fmk group, "*" indicates a significant difference between GHSC-74 group and control group, as analyzed by Student's *t*-test (##$p < 0.01$). (C) Translocation of AIF was analyzed by observing its release from the mitochondria and translocation to the nucleus by immunofluorescence microscopy. HepG2 cells were treated with GHSC-74 (4 μM) for 0, 24 and 48 h, incubated with antibody against AIF, and then labeled with Cy3-conjugated secondary antibody. The nuclei are stained with DAPI. Purple, nuclear translocation of AIF is shown by overlap of AIF (red fluorescence) and nuclear staining (blue fluorescence) (magnification 200×). (D) Western blot analysis showed that AIF decreased correspondingly in the mitochondrial fractions treated with GHSC-74, where total protein was used as a control for the amount of protein loaded. (E) GHSC-74-induced caspase-independent pathway was mediated by AIF translocation. HepG2 cells were treated with GHSC-74 (4 μM) in the presence or absence of z-VAD-fmk (80 μM), incubated with antibody against AIF, and then labeled with Cy3-conjugated secondary antibody. The nuclei are stained with DAPI. Purple, nuclear translocation of AIF is shown by overlap of AIF (red fluorescence) and nuclear staining (blue fluorescence) (magnification 200×). (For interpretation of the references to color in this figure legend, the reader is referred to the web version of the article.).

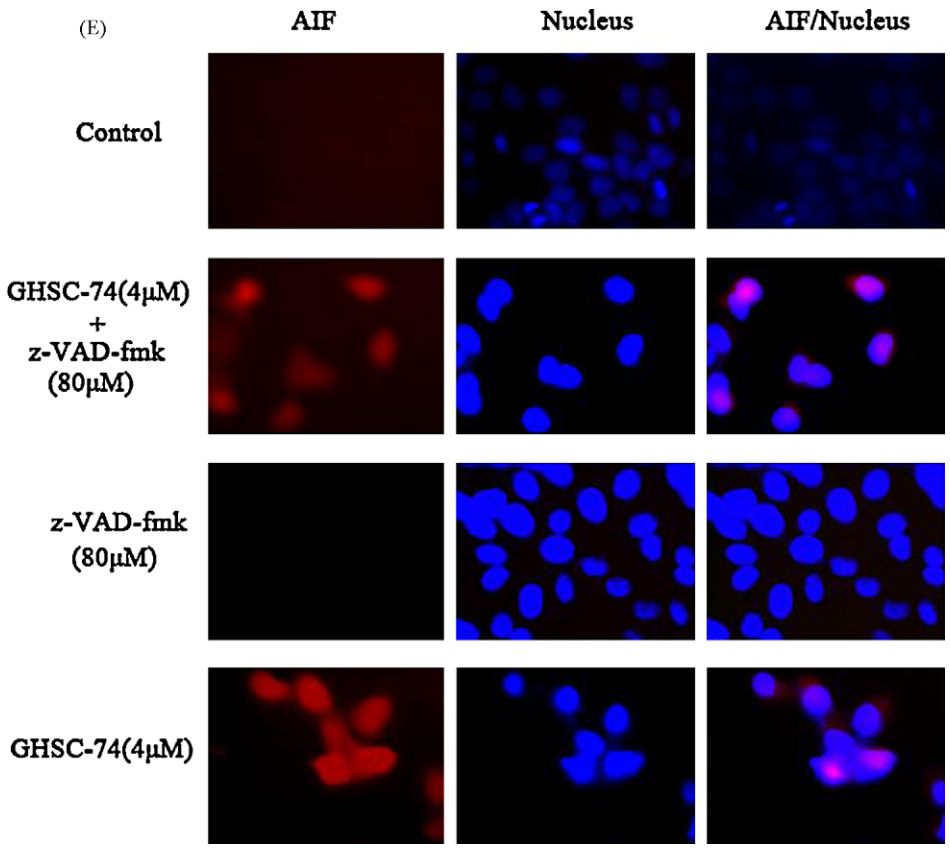

Fig. 5. (*Continued*).

HepG2 cells were leveled with the cationic lipophilic dye JC-1 and accumulated within the mitochondria in a potential-dependent manner. When the mitochondrial membrane potential was disrupted, the fluorescence emission of JC-1 dye changed from red to green. HepG2 cells were treated with GHSC-74 (4 μM) for different time periods, harvested, stained with JC-1, and analyzed by flow cytometry. As shown in Fig. 4, treatment of HepG2 cells with GHSC-74 resulted in a time-dependent increase in the number of green fluorescence$^+$ cells from 3.2 ± 0.4% in non-GHSC-74-treated cells to 5.4 ± 0.5% and 11.8 ± 1.1% (Fig. 4B), respectively by 4 μM concentration of GHSC-74 treatment for 24 h and 48 h, while a time-dependent decrease in the number of red fluorescence$^+$ cells was observed (Fig. 4C). These data suggested that treatment of HepG2 cells with GHSC-74-induced disruption of the mitochondrial membrane potential.

3.4. GHSC-74 induces apoptosis of HepG2 cells through mitochondrial disruption including both caspase-dependent and-independent pathways

To confirm the role of caspase activation in GHSC-74-induced apoptosis of HepG2 cells, we treated HepG2 cells with the broad-spectrum caspase inhibitor, z-VAD-fmk, 1 h before adding GHSC-74 at 4 μM for a further 48 h. Fig. 5A and B shows that while z-VAD-fmk completely inhibited activity of caspase-9 induced by GHSC-74, it only partially blocked GHSC-74-induced apoptosis. These results suggest that both caspase-dependent and -independent pathways were induced by GHSC-74 in HepG2 cells. In addition, caspase-9 activation also shows Cytochrome c released from the mitochondria may be involved in GHSC-74-induced apoptosis in HepG2 cells.

As AIF is involved in induction of apoptotic cell death through caspase-independent pathway [21,23], we examined whether AIF played a role in GHSC-74-induced apoptotic cell death. Translocation of AIF was analyzed by observing its release from the mitochondria and translocation to the nucleus by immunofluorescence microscopy. As shown in Fig. 5C, immunofluorescence microscopy showed that AIF was translocated into the nucleus and caused nuclear condensation after treatment with GHSC-74 (4 μM) for 24 h and 48 h. Western blot analysis showed that AIF was localized exclusively in mitochondrial fractions before treatment, but after exposure to GHSC-74 for 12 h, AIF decreased correspondingly in the mitochondrial fractions (Fig. 5D). In addition, caspase inhibitor z-VAD-fmk did not affect AIF translocation into the nucleus after GHSC-74 treatment (Fig. 5E). These results suggest that GHSC-74-induced apoptotic cell death in HepG2 cells was partially mediated by AIF translocation from the mitochondria into the nucleus via a caspase-independent pathway.

3.5. Fas/FasL interaction does not mediate GHSC-74-triggered apoptosis

To assess whether the death receptor pathway was also involved in GHSC-74-induced apoptosis, we next checked whether the protein expression of Fas and FasL, which are representative members of the death receptor pathway, was influenced by GHSC-74. Interestingly, flow cytometric analysis using anti-Fas-specific antibody and anti-FasL-specific antibody revealed that Fas and FasL level was not increased in GHSC-74-treated cells compared with the untreated controls (Fig. 6), suggesting that GHSC-74-induced apoptosis in HepG2 cells without triggering the Fas/FasL system.

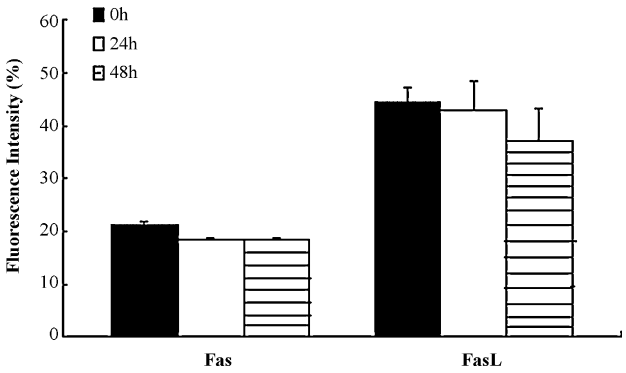

Fig. 6. Flow cytometry analysis of Fas and FasL expression in HepG2 cells. After incubation with GHSC-74 (4 μM) for 0 h, 24 h and 48 h, cells were stained with FITC-conjugated anti-Fas-specific antibody or PE—conjugated anti-FasL-specific antibody. Fas and FasL expression was analyzed by flow cytometry as described previously. The percentage of FITC-positive or PE-positive cells is indicated. The experiment was performed in triplicate in three separate experiments ad the results are expressed as mean ± S.D.

3.6. GHSC-74-induced apoptosis of HepG2 cells is partially dependent of the generation of ROS

Numerous investigations have documented that oxidative stress-mediated cellular changes are frequently induced in cells exposed to cytotoxic drugs, UV, or γ-irradiation [31,32], and ROS is a mediator of caspase-independent cell death [33]. The present study examined involvement of ROS in GHSC-74-induced effect in HepG2 cells. Intracellular ROS level was measured using the fluorescent probe DCFH/DA. This cell-permeable dye, once inside the cells, is cleaved by endogenous esterase into DCFH. The intracellular nonfluorescent form of DCFH is oxidized, commonly by hydrogen peroxide, into the fluorescent form, 2′,7′-dichlorofluorescein (DCF). Fluorescence intensity was measured after treatment with a 4 μM concentration of GHSC-74 for various time courses. Fig. 7A showed that GHSC-74 increased mean DCF fluorescence markedly in a time-dependent manner and treatment of cells with GHSC-74 (4 μM) for 48 h caused a 2.9-fold increase in mean DCF fluorescence.

To study if increased production of ROS may play a role in GHSC-74-induced apoptosis of HepG2 cells, we treated HepG2 cells with the antioxidant, NAC, 1 h before adding GHSC-74 for a further 48 h. Fig. 7C shows that pretreatment with NAC partially prevents GHSC-74-induced increase in sub-G1 population, while it markedly decreased GHSC-74-induced production of ROS (Fig. 7B). However, increase in intracellular ROS was not required for AIF translocation (Fig. 7D). These results suggest that GHSC-74-induced apoptosis was mediated by ROS-dependent apoptosis pathway and ROS-independent AIF translocation.

4. Discussion

Many efforts have been made to search for compounds that can influence apoptosis and understand mechanisms of their actions. In recent years, more knowledge has been obtained about how cardiac glycosides induce cell death in human cancers. GHSC-74 is a cardiac glycoside isolated from the seeds of *C. manghas* L. In the previous study, we have demonstrated that GHSC-74 reduced the viability of HepG2 cells in a time- and dose-dependent manner [28]. Flow cytometric analysis and mitotic index assay in our study showed that GHSC-74 could cause S and G2 phase arrest in a time-dependent manner (Fig. 2A–C). A significant time-dependent increase in the percentage of sub-G1 cells suggested that apoptosis was involved in GHSC-74-induced cell death (Fig. 3A). In addition to an increase in sub-G1 cells, apoptosis was confirmed by DNA fragmentation analysis and characteristic morphological changes, including membrane blebbling, cell shrinkage, chromatin condensation, and formation of apoptotic bodies [34]. DAPI staining clearly showed condensed and fragmented nuclei and apoptotic bodies in HepG2 cells treated with GHSC-74 (Fig. 3C). Cleavage of DNA at the internucleosomal linker sites yielding DNA fragments in multiples fragments (180–200 bp) is regarded as a biochemical hallmark of apoptosis dependent on caspase activation [35]. At the same time, on induction of apoptosis, AIF is translocated to the nucleus and causes large-scale DNA fragmentation and chromatin condensation in a caspase-independent manner [23]. We presume because caspase-dependent and -independent pathways were involved in GHSC-74-induced apoptosis of HepG2 cells, the DNA ladder is not evident when fragmented DNA from GHSC-74-treated cells was separated by agarose gel electrophoresis (Fig. 3B). In this study, our focus was on cellular mechanisms whereby GHSC-74-induced cell cycle arrest and apoptosis in HepG2 cells.

Effective anticancer therapies (chemotherapeutic agents and ionizing radiation) kill proliferating cancer cells by damaging their DNA and inducing apoptosis. It is known that cell cycle dysregulation is a hallmark of tumor cells. Regulation of proteins that mediate critical events of the cell cycle may be a useful anti-tumor target [36]. Cellular response to DNA damage involves cell cycle arrest, mainly at G1 and G2 phases. Cell cycle arrest allows cells to repair the damage before entering S-phase for DNA replication and M-phase for mitosis, which is critical for cells to maintain their genetic integrity. Failure to repair DNA damage would cause mutations and eventually cell death. S and G2 arrest following DNA damage has been associated with accumulation of hyperphosphorylated and relatively inactive CDC2/cyclin B complexes [37,38], and in some instances basal levels of cyclin B1 have been shown to decrease subsequent DNA damage [39]. S and G2 phase arrest of the cell cycle as observed in the present study could be considered as an additional pathway to suppress the growth of HepG2 cells and explain the inhibitory effect of GHSC-74 on cell growth (Fig. 2A–C). GHSC-74-induced S and G2 phase arrest in HepG2 cells was accompanied by alteration in CDC2 and cyclin B1 protein levels (Fig. 2D).

Two major apoptotic pathways, the death receptor pathway and the mitochondrial apoptotic pathway, are well characterized in mammalian cells [16]. To address the question of the apoptotic pathway that becomes activated in response to GHSC-74, we firstly analyzed the death receptor pathway, which is known to be triggered by members of the death receptor family, such as Fas receptor and tumor necrosis factor receptor [18]. The physiological role of the Fas/FasL pathway outside the immune system remains unclear, although a role for the Fas system has been suggested in drug-induced apoptosis in some cell types [40,41]. Our data showed that the protein levels of Fas and FasL were not increased in GHSC-74-treated cells compared with the untreated controls (Fig. 6). Therefore, we concluded that GHSC-74-induced apoptosis in HepG2 cells without triggering the Fas/FasL (CD95/CD178) system. However, whether other death receptors are involved in GHSC-74-induced HepG2 apoptosis awaits results of more experiments.

We also determined whether GHSC-74-induced apoptosis via the mitochondrial apoptotic pathway. In mammals, mitochondria act as central checkpoints for many forms of apoptosis. The mitochondrial pathway is thought to be the principal target of the survival signaling system [19,22]. Mitochondria commit apoptosis via increased permeability of the outer mitochondrial membrane, decreased mitochondrial transmembrane potential ($\Delta\Psi_m$), release of cytochrome c (Cyt c) and AIF, and production of ROS. As shown in Fig. 4, treatment of HepG2 cells with 4 μM GHSC-74 for different time courses resulted in a time-dependent increase in the number of green fluorescence-positive cells, indicating that the mitochondrial membrane was depolarized. Fig. 5A and B shows that while z-VAD-fmk completely inhibited activity of caspase-9

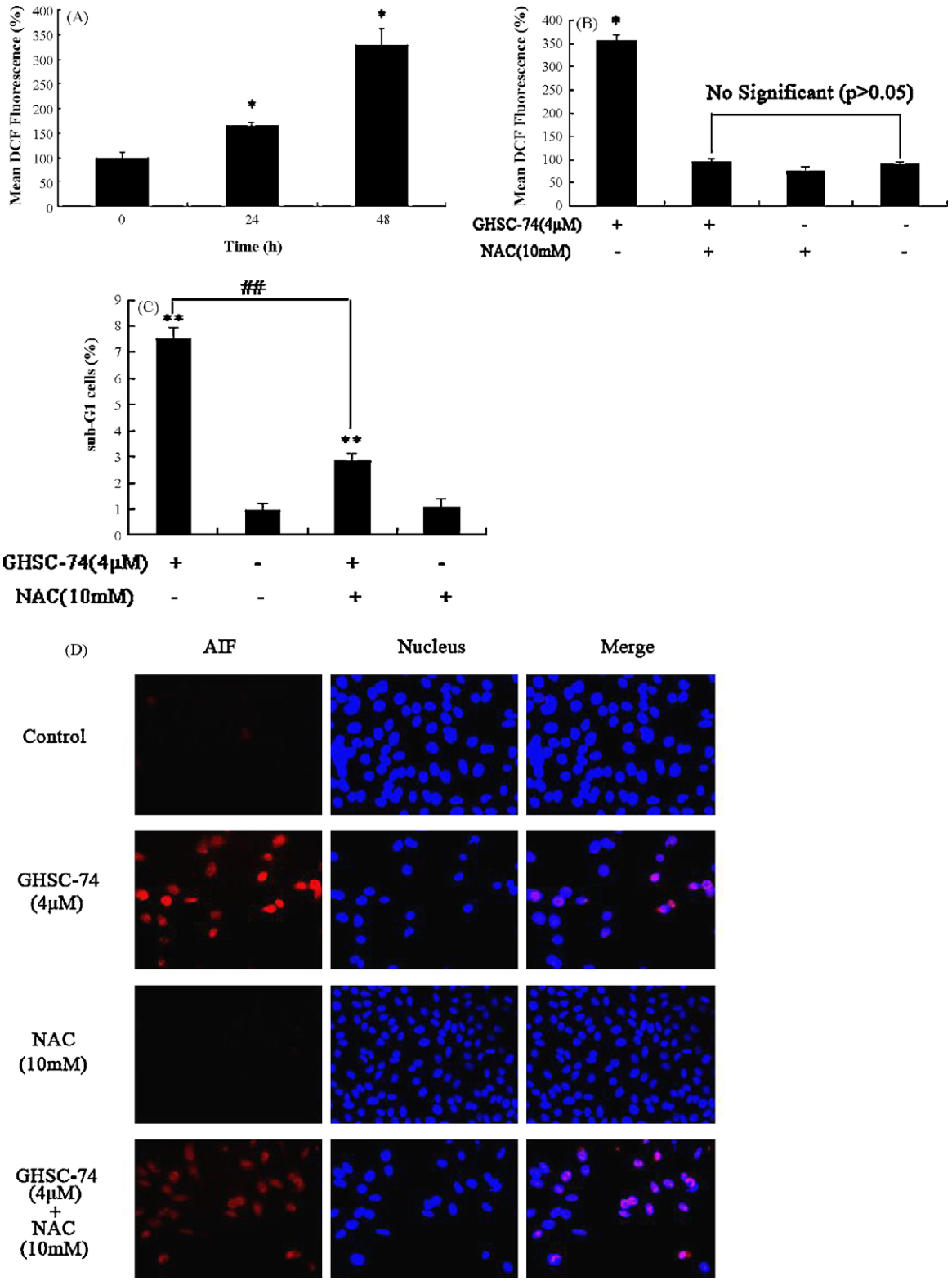

Fig. 7. Increase in intracellular ROS was involved in GHSC-74-induced apoptosis, but not required for AIF translocation. (A) Elevation of intracellular ROS level after GHSC-74 treatment. HepG2 cells were treated with GHSC-74 (4 μM) for indicated time courses and then loaded with DCFH/DA. The percentage of mean DCF fluorescence was measured by flow cytometry. Each value is the mean ± S.D. of three determinations. The asterisk indicates a significant difference between control and GHSC-74-treated cells as analyzed by Student's *t*-test (*$p < 0.05$, **$p < 0.01$). (B) The antioxidant NAC inhibited the generation of ROS induced by GHSC-74. HepG2 cells were treated with NAC (10 mM) for 1 h before adding GHSC-74 (4 μM) for another 48 h. ROS production was measured as described in (A). (C) The antioxidant NAC partially inhibited GHSC-74-induced apoptosis. HepG2 cells were treated with NAC for 1 h before adding GHSC-74 (4 μM) for another 48 h. Apoptosis was measured by the PI method using flow cytometry. "#" indicates a significant difference between GHSC-74 group and GHSC-74+NAC group, as analyzed by Student's *t*-test (##$p < 0.01$). (D) Increase in intracellular ROS was not required for AIF translocation. HepG2 cells were treated with NAC (10 mM) for 1 h before adding GHSC-74 (4 μM) for another 48 h, incubated with antibody against AIF, and then labeled with the Cy3-conjugated secondary antibody. The nuclei are stained with DAPI. Purple, nuclear translocation of AIF is shown by overlap of AIF (red fluorescence) and nuclear staining (blue fluorescence) (magnification 200×). (For interpretation of the references to color in this figure legend, the reader is referred to the web version of the article.).

induced by GHSC-74, it only partially blocked GHSC-74-induced apoptosis. These results suggest that both caspase-dependent and -independent pathways were induced by GHSC-74 in HepG2 cells. In addition, caspase-9 activation also shows Cytochrome c released from the mitochondria may be involved in GHSC-74-induced apoptosis in HepG2 cells. It is reported [21,23] that AIF mediates apoptosis through a caspase-independent pathway. Mitochondrial AIF translocates to the nucleus on death stimuli and initiates nuclear condensation, leading to large-scale chromatin fragmentation and subsequent apoptosis. Immunofluorescence microscopy showed that AIF translocated into the nucleus in HepG2 cells (Fig. 5C), which was not inhibited by z-VAD-fmk (Fig. 5E). At the same time, AIF decreased correspondingly in the mitochondrial fractions after exposure to GHSC-74 for 12 h (Fig. 5D). These results suggest that activation of the caspase-independent apoptotic pathway mediated via AIF translocation into the nucleus was involved in GHSC-74-induced HepG2 apoptosis.

Reactive oxygen species are important mediators and regulators of apoptosis. Various apoptosis stimuli such as tumor necrosis factor, irradiation, and chemicals such as etoposide may increase the level of intracellular ROS [42,43]. Apoptosis can be abolished by antioxidants [44] and induced by treatment with ROS such as H_2O_2 [45]. GHSC-74 exposure increased ROS accumulation in a time-dependent manner (Fig. 7A), and Fig. 7C shows that pretreatment with NAC partially prevent GHSC-74-induced increase of sub-G1 population, while it markedly decreased GHSC-74-induced production of ROS (Fig. 7B), indicating that ROS-independent and ROS-dependent apoptotic pathways were involved in GHSC-74-mediated cell death. However, pre-incubation with NAC did not prevent nuclear translocation of AIF (Fig. 7D), implying that increase in intracellular ROS was not required for AIF translocation. From these results, firstly, we presume that ROS generation may be not involved in mitochondrial disruption, thus pre-incubation with NAC did not prevent nuclear translocation of AIF. ROS also are link signaling pathway leading to cell death through the mitogen-activated protein kinase pathway [46], the nuclear factor κB pathway [47], or apoptosis signal-regulating kinase 1[48]. Secondly, we presume that ROS-independent PARP-1 activation that mediated nuclear translocation of AIF was involved in GHSC-74-mediated cell death. Poly-adenosine diphosphate (ADP)-ribose polymerase 1 (PARP-1), the most abundant protein of the poly (ADP-ribose) polymerase family members, is rapidly activated by DNA damage. PARP-1 activation also affects mitochondria membrane potential loss and subsequent AIF release [49]. However, whether two hypotheses are reasonable awaits results of more experiments.

In summary, GHSC-74 inhibited growth of HepG2 cells by inducing S and G2 arrest of the cell cycle and by triggering apoptosis. S and G2 phase arrest was likely mediated by down-regulation of CDC2 and Cyclin B1 proteins. GHSC-74-induced apoptosis via mitochondrial disruption including both caspase-dependent and -independent pathways, and ROS generation.

Conflict of interest

None.

Acknowledgment

This work was supported by National Ocean 863 Project of the Ministry of Science and Technology of China (# 2006AAD9Z447).

References

[1] F. Abe, T. Yamauchi, Studies on Cerbera. I. Cardiac glycosides in the seeds, bark, and leaves of *Cerbera manghas* L, Chem. Pharm. Bull. 25 (1977) 2744–2748.
[2] E. Braunwald, Effects of digitalis on the normal and the failing heart, J. Am. Coll. Cardiol. 5 (1985) 51A–59A.
[3] S. Wilhelm, S.B. Georgios, Endogenous and exogenous cardiac glycosides: their roles in hypertension, salt metabolism, and cell growth, Am. J. Physiol. Cell Physiol. 293 (2007) C509–C536.
[4] F. Steffen, F.S. Manuela, A. Anne-Catherine, M. Daniela, Z. Beatrice, A.S. Ralph, Cardiac glycosides initiate Apo2L/TRAIL-induced apoptosis in non–small cell lung cancer cells by up-regulation of death receptors 4 and 5, Cancer Res. 66 (2006) 5867–5874.
[5] D.M. Parkin, F. Bray, J. Ferlay, P. Pisani, Global cancer statistics, 2002, CA, Cancer J. Clin. 55 (2005) 74–108.
[6] F.X. Bosch, J. Ribes, M. Diaz, R. Cleries, Primary liver cancer: worldwide incidence and trends, Gastroenterology 127 (2004) S5–S16.
[7] R.T. Poon, S.T. Fan, C.M. Lo, I.O. Ng, C.L. Liu, C.M. Lam, J. Wong, Improving survival results after resection of hepatocellular carcinoma: a prospective study of 377 patients over 10 years, Ann. Surg. 234 (2001) 63–70.
[8] M. Schwartz, Liver transplantation for hepatocellular carcinoma, Gastroenterology 127 (2004) S268–S276.
[9] D.K. Orren, L.N. Petersen, V.A. Bohr, Persistent DNA damage inhibits S-phase and G2 progression, and results in apoptosis, Mol. Biol. Cell 8 (1997) 1129–1142.
[10] L. Gamet-Payrastre, P. Li, S. Lumeau, G. Cassar, M.A. Dupont, S. Chevolleau, N. Gasc, J. Tulliez, F. Tercé, Sulforaphane, a naturally occurring isothiocyanate, induces cell cycle arrest and apoptosis in HT29 human colon cancer cells, Cancer Res. 60 (2000) 1426–1433.
[11] P.M. O'Connor, D.K. Ferris, M. Pagano, G. Draetta, J. Pines, T. Hunter, D.L. Longo, K.W. Kohn, G2 delay induced by nitrogen mustard in human cells affects cyclinA/cdk2, and cyclin B1/cdc-2 kinase complexes differently, J. Biol. Chem. 268 (1993) 8298–8308.
[12] A.W. Murray, Revisiting the cell cycle: cyclins revisited, Cell 116 (2004) 221–234.
[13] B. Lewin, Driving the cell cycle: M phase kinases, its partners, and substrates, Cell 61 (1990) 743–752.
[14] M. Doree, S. Galas, The cyclin-dependent protein kinases and the control of cell division, FASEB J. 8 (1994) 1114–1121.
[15] L.L. Parker, H. Piwnica-Worms, Inactivation of the p34cdc2-cyclin B complex by the human WEE1 tyrosine kinase, Science 257 (1992) 1955–1957.
[16] M.O. Hengartner, The biochemistry of apoptosis, Nature 407 (2000) 770–776.
[17] N. Itoh, S. Yonehara, A. Ishii, M. Yonehara, S. Mizushima, M. Sameshima, A. Hase, Y. Seto, S. Nagata, The polypeptide encoded by the cDNA for human cell surface antigen Fas can mediate apoptosis, Cell 66 (1991) 233–243.
[18] D. Wallach, E.E. Varfolomeev, N.L. Malinin, Y.V. Goltsev, A.V. Kovalenko, M.P. Boldin, Tumor necrosis factor receptor and Fas signaling mechanisms, Annu. Rev. Immunol. 17 (1999) 331–367.
[19] M. Crompton, The mitochondrial permeability transition pore and its role in cell death, Biochem. J. 341 (1999) 233–249.
[20] P. Li, D. Nijhawan, I. Budihardjo, S.M. Srinivasula, M. Ahmad, E.S. Alnemri, X. Wang, Cytochrome c and dATP-dependent formation of Apaf-1/caspase-9 complex initiates an apoptotic protease cascade, Cell 91 (1997) 479–489.
[21] S.A. Susin, H.K. Lorenzo, N. Zamzami, I. Marzo, B.E. Snow, G.M. Brothers, J. Mangion, E. Jacotot, P. Costantini, M. Loeffler, N. Larochette, D.R. Goodlett, R. Aebersold, D.P. Siderovski, J.M. Penninger, G. Kroemer, Molecular characterization of mitochondrial apoptosis-inducing factor, Nature 397 (1999) 441–446.
[22] G. Kroemer, J.C. Reed, Mitochondrial control of cell death, Nat. Med. 6 (2000) 513–519.
[23] N. Joza, S.A. Susin, E. Daugas, W.L. Stanford, S.K. Cho, C.Y.J. Li, T. Sasaki, A.J. Elia, H.Y. Mary Cheng, L. Ravagnan, K.F. Ferri, N. Zamzami, A. Wakeham, R. Hakem, H. Yoshida, Y.Y. Kong, T.W. Mak, J.C. Zunigapflucker, G. Kroemer, J.M. Penninger, Essential role of the mitochondrial apoptosis-inducing factor in programmed cell death, Nature 410 (2001) 549–554.
[24] V.J. Thannickal, B.L. Fanburg, Reactive oxygen species in cell signaling, Am. J. Physiol. Lung Cell Mol. Physiol. 279 (2000) L1005–L1028.
[25] C.P. Baran, M.M. Zeigler, S. Tridandapani, C.B. Marsh, The role of ROS and RNS in regulating life and death of blood monocytes, Curr. Pharm. Des. 10 (2004) 855–866.
[26] C. Bubici, S. Papa, C.G. Pham, F. Zazzeroni, G. Franzoso, The NFkappaB-mediated control of ROS and JNK signaling, Histol. Histopathol. 21 (2006) 69–80.
[27] K. Kannan, S.K. Jain, Oxidative stress and apoptosis, Pathophysiology 7 (2000) 153–163.
[28] B. Feng, C.G. Huang, R.H. Chen, Y.W. Guo, B.H. Jiao, 2′-epi-2′-*O*-acetylthevetin B induces apoptosis partly via Ca^{2+}-mediated mitochondrial pathway in human hepatocellular carcinoma HepG2 cells, Cell Biol. Int. 33 (2009) 918–925.
[29] Y.W. Han, S.Z. Kim, S.H. Kim, W.H. Park, The changes of intracellular H_2O_2 are an important factor maintaining mitochondria membrane potential of antimycin A-treated As4.1 juxtaglomerular cells, Biochem. Pharmacol. 73 (2007) 863–872.
[30] X.D. Zhang, X.Y. Zhang, C.P. Gray, T. Nguyen, P. Hersey, Tumor necrosis factor-related apoptosis-inducing ligand-induced apoptosis of human melanoma is regulated by Smac/DIABLO release from mitochondria, Cancer Res. 61 (2001) 7339–7348.
[31] J. Wen, K.R. You, S.Y. Lee, C.H. Song, D.G. Kim, Oxidative stress-mediated apoptosis. The anticancer effect of the sesquiterpene lactone parthenolide, J. Biol. Chem. 277 (2002) 38954–38964.
[32] X. Sheng-Tanner, E.A. Bump, D.W. Hedley, An oxidative stress-mediated death pathway in irradiated human leukemia cells mapped using multilaser flow cytometry, Radiat. Res. 150 (1998) 636–647.

[33] C. Fleury, B. Mignotte, J.L. Vayssiere, Mitochondrial reactive oxygen species in cell death signaling, Biochimie 84 (2002) 131–141.
[34] S. Rello, J. Stockert, V. Moreno, A. Gamez, M. Pacheco, A. Juarranz, M. Canete, A. Villanueva, Morphological criteria to distinguish cell death induced by apoptotic and necrotic treatments, Apoptosis 10 (2005) 201–208.
[35] H. Steller, Mechanisms and genes of cellular suicide, Science 267 (1995) 1445–1449.
[36] Z.A. Stewart, M.D. Westfall, J.A. Pietenpol, Cell-cycle dysregulation and anticancer therapy, Trends Pharmacol. Sci. 24 (2003) 139–145.
[37] P.M. O'Connor, D.K. Ferris, I. Hoffmann, J. Jackman, G. Draetta, K.W. Kohn, Role of the cdc25C phosphatase in G2 arrest induced by nitrogen mustard, Proc. Natl. Acad. Sci. U.S.A. 91 (1994) 9480–9484.
[38] R.B. Lock, Inhibition of $p34^{cdc2}$ kinase activation, $p34^{cdc2}$ Tyrosine dephosphorylation, and mitotic progression in Chinese hamster ovary cells exposed to etoposide, Cancer Res. 52 (1992) 1817–1822.
[39] G.D. Kao, W.G. McKenna, A. Maity, K. Blank, R.J. Muschel, Cyclin B1 availability is a rate-limiting component of the radiation-induced G2 delay in HeLa cells, Cancer Res. 57 (1997) 753–758.
[40] D.M. Tillman, I. Petak, J.A. Houghton, A Fas-dependent component in 5-fluorouracil/leucovorin-induced cytotoxicity in colon carcinoma cells, Clin. Cancer Res. 5 (1999) 425–430.
[41] M. Muller, S. Strand, H. Hug, E.M. Heinemann, H. Walczak, W.J. Hofmann, W. Stremmel, P.H. Krammer, P.R. Galle, Drug-induced apoptosis in hepatoma cells is mediated by the CD95(APO-1/Fas) receptor/ligand system and involves activation of wildtype p53, J. Clin. Investig. 99 (1997) 403–413.
[42] J.W. Larrick, S.C. Wright, Cytotoxic mechanism of tumor necrosis factor-α, FASEB J. 4 (1990) 3215–3223.
[43] Y. Manome, R. Datta, N. Taneja, T. Shafman, E. Bump, R. Hass, R. Weichselbaum, D. Kufe, Coinduction of c-jun gene expression and internucleosomal DNA fragmentation by ionizing radiation, Biochemistry 32 (1993) 10607–10613.
[44] A. Cossarizza, C. Franceschi, D. Monti, S. Salvioli, E. Bellesia, R. Rivabene, L. Biondo, G.R.A. Tinari, W. Malorni, Protective effect of N-acetylcysteine in tumor necrosis factor-α-induced apoptosis in U937 cells: the role of mitochondria, Exp. Cell Res. 220 (1995) 232–240.
[45] A. Dumont, S.P. Hehner, T.G. Hofmann, M. Ueffing, W. Droge, M.L. Schmitz, Hydrogen peroxide-induced apoptosis is CD95-independent, requires the release of mitochondria-derived reactive oxygen species and the activation of NF-kB, Oncogene 18 (1999) 747–757.
[46] C Yu, M. Rahmani, P. Dent, S. Grant, The hierarchical relationship between MAPK signaling and ROS generation in human leukemia cells undergoing apoptosis in response to the proteasome inhibitor Bortezomib, Exp. Cell Res. 295 (2004) 555–566.
[47] C.G. Pham, C. Bubici, F. Zazzeroni, S. Papa, J. Jones, K. Alvarez, S. Jayawardena, E. Desmaele, R. Cong, C. Beaumont, Ferritin heavy chain upregulation by NF-kappa B inhibits TNFalpha-induced apoptosis by suppressing reactive oxygen species, Cell 119 (2004) 529–542.
[48] H. Kadowaki, H. Nishitoh, F. Urano, C. Sadamitsu, A. Matsuzawa, K. Takeda, H. Masutani, J. Yodoi, Y. Urano, T. Nagano, Amyloid beta induces neuronal cell death through ROS-mediated ASK-1 activation, Cell Death Differ. 12 (2005) 19–24.
[49] P. Moon-Taek, K. Min-Jung, K. Young-Hee, Choi Soon-Young, L. Jae-Hoon, C. Jung-A, K. Chang-Mo, C. Chul-Koo, K. Seongman, B. Sangwoo, L. Yun-Sil, Y.C. Hee, L. Su-Jae, Phytosphingosine in combination with ionizing radiation enhances apoptotic cell death in radiation-resistant cancer cells through ROS-dependent and -independent AIF release, Blood 105 (2005) 1724–1733.